General Disclaimer

One or more of the Following Statements may affect this Document

- This document has been reproduced from the best copy furnished by the organizational source. It is being released in the interest of making available as much information as possible.

- This document may contain data, which exceeds the sheet parameters. It was furnished in this condition by the organizational source and is the best copy available.

- This document may contain tone-on-tone or color graphs, charts and/or pictures, which have been reproduced in black and white.

- This document is paginated as submitted by the original source.

- Portions of this document are not fully legible due to the historical nature of some of the material. However, it is the best reproduction available from the original submission.

NASA TECHNICAL MEMORANDUM

NASA TM 77789

THERMAL INVESTIGATION OF AN ELECTRICAL HIGH-CURRENT ARC
WITH POROUS, GAS-COOLED ANODE

E.R.G. Eckert, P.A. Schoeck and R.F. Winter

NATIONAL AERONAUTICS AND SPACE ADMINISTRATION
WASHINGTIN, D.C. 20546,   DECEMBER, 1984

1. Report No. NASA-TM-77789	2. Government Accession No.	3. Recipient's Catalog No.
4. Title and Subtitle Thermal Investigation of an Electrical High-Current Arc with Porous Gas-Cooled Anode		5. Report Date December, 1984
		6. Performing Organization Code
7. Author(s) Ernst R.G. Eckert, Peter A. Schoeck and Edgar R.F. Winter		8. Performing Organization Report No.
		10. Work Unit No.
9. Performing Organization Name and Address Leo Kanner Associates P.O. Box 5187 Redwood City CA 94063		11. Contract or Grant No. NASA-4005
		13. Type of Report and Period Covered Translation
12. Sponsoring Agency Name and Address NATIONAL AERONAUTICS AND SPACE ADMINISTRATION WASHINGTON, D.C. 20546		14. Sponsoring Agency Code

15. Supplementary Notes

16. Abstract

The following quantities have been measured on a high-intensity electric arc with tungsten cathode and transpiration cooled graphite, anode burning in argon:electric current and voltage, cooling-gas flow rate (argon), and surface temperature of the anode and of the anode holder and temperature profile in three cross-sections of the arc column. The last-mentioned values were obtained from spectroscopic photographs. From the measured quantities, the following values were calculated: the heat flux into the anode surface, the heat loss of the anode by radiation and conduction, and the heat which was regeneratively transported by the cooling gas back into the arc space. Heat balances for the anode were also obtained. The anode losses (which are approximately 80% of the total arc power for free burning arcs) were reduced by transpiration cooling to 20%. The physical processes of the energy transfer from the arc to the anode are discused qualitatively.

17. Key Words (Selected by Author(s))		18. Distribution Statement Unclassified - Unlimited	
19. Security Classif. (of this report) Unclassified	20. Security Classif. (of this page) Unclassified	21. No. of Pages 26	22.

Symbols

A_m^n,   Transition probability of the line;

$E_m k$ Excitation energy of the line;

F,   Anode surface;

F_h,   External surface of the anode holder;

g_m,   Statical weight of the excitation turn of the line;

h Planck's constant;

I,   Electrical current intensity;

I_L,   Intensity of a spectral line;

I_1,   Enthalphy of the cooling gas at the cathode spot temperature T_1;

I_2,   Enthalpy of the cooling gas at the entrance T_0;

k,   Boltzmann's constant;

L,   Layer thickness of the heater;

$\dot{m}$,   Mass flow of the cooling gas (argon);

n^-,   Particle density of the electrons;

n^+,   Particle density of the ions;

n,   Particle density;

$\dot{n}^-$,   Particle flow of the electrons per unit of area;

$\dot{n}^+$,   Particle density of the ions per unit of area;

$\dot{n}_s^-$,   Particle flow of the electrons formed by ionization per unit of area;

Q_a,   Heat flow from the arc to anode surface;

Q_g,   Perceptible heat of the arc plasma plus about 4% cathode losses;

Q_k,   Heat absorbtion of the cooling gas in the anode;

Q_i Heat loss through the anode holder;

Q_0,   Electrical arc power;

Q_s,   Radiation losses of the anode;

r,   Radial distance from the arc axis;

R,   Arc radius;

s,   Thickness of the anode;

T,   Absolute temperature;

T_0,   Temperature of inflow of cooling gas to the anode holder;

T_1,   Surface temperature of the spot;

T_2,   Average anode surface temperature outside of the focal spot;

U,   Electrical drop of voltage between the electrodes;

v^-,   Velocity of drift of the electrons;

v^+,   Velocity of drift of the ions;

$\bar{v}$,   Average outlet velocity of the cooling gas from anode (referred to the anode surface);

x,   Ratio of the focal spot area to the anode area;

$z_0^{(i)}$, Partial function of the excitation

Greek symbols

ϵ Emissions capacity of the anode and the anode holder;

η Coordinate (See Fig 13);

λ Coefficient of thermal conductivity of the anode holders;

υ Frequency of the line;

σ Stefan-Boltzmann constant

ξ Distance from the optical axis;

ζ Loss coefficient of the anode.

THERMAL INVESTIGATION OF AN ELECTRICAL HIGH-CURRENT ARC WITH POROUS, GAS-COOLED ANODE[1]

Ernst R.G. Eckert, Peter A. Schoeck, and Edgar R.F. Winter

University of Minnesota, Heat Transfer Laboratory
Minneapolis

Introduction

A new area of application has been found most recently for the   /296*
electrical arc, inasmuch as it is used to heat gases to temperatures
on the order of 10,000°C. At such high temperatures a part of the
atoms are split into electrons and ions, and thus the gas becomes
electrically conductive. These gases, called plasmas, are expanded
in wind tunnels, in which an attempt is made to imitate the conditions
which a spacecraft returning to the atmosphere or a missile will find.
Moreover they are used for propulsion in rockets, or to produce
electricity in generators without rotating parts. For these appli-
cations, we are interested in feeding the greatest possible fraction
of the electrical energy converted in the arc to the heated gases.
On the other hand in modern plants, which are mostly operated with
water-cooled copper anodes, often more than half of the power supplied
as heat is lost in the cooling water of the anode and the walls of
the container in which the arc burns. The first loss can be reduced
to a considerable extent by manufacturing the anode of a porous
material and allowing a cooling gas to pass through the pores into
the combustion chamber. This cooling process which has already

*Numbers in margins indicate pagination in foreign text.

1

been used in technology for several years for other purposes and known
as transfiguration cooling was to our knowledge applied for the
first time for anode cooling by Sheer /1/. The purpose of this
investigation, on which a partial record is given in this article,
is to determine the thermal conditions in a porous, gas-cooled anode
and in the neighboring zone of the arc, to obtain the heat balance of
the anode and to explain the mechanism of heat transfer on the anode.
The investigation concerned primarily a high current arc burning in
argon, so as not to allow the number of the parameters determining
the process to become too large.

Experimental Equipment and Measurement Program

Figure 1 shows the experimental equipment in its main parts.
The arc burns between the cathode (a), a bar of tungsten of 6 mm in
diameter, ending at the top in a cone with 45° aperature angle and
whose other end is inserted in a water-cooled copper holder (b),
and anode which consists of porous graphite of the type NC 60 of
National Carbon Company (Division of Union Carbide Corporation) USA.
The anode (c) is in the shape of a disk, with a diameter of 12.5mm
and is 5 mm thick with a porosity of 50 percent and a pore diameter
of about 30 microns. The disk is connected with a graphite holder
(d) to the cooper anode head (e), which is used simultaneously to feed
the cooling gas (argon) flow. The graphite holder is designed in
such a way that heat losses by dissipation are kept as small as possible
and can be measured with high precision. For this reason the aluminum
disk (f) is also provided which keeps the arc radiation and convection
flows away from the holder. A slow flow of argon is blown in through
an annular area (g) surrounding the cathode holder. It was established
with preliminary experiments that air is thus kept far from the arc.
The spectrographic measurements to be discussed later were carried
out with a similar experimental equipment, except that the anode disk
was 12mm thick, and the graphite holder was replaced by a water-cooled
copper holder. The latter anode with its holder is shown in the   /297
upper portion of Fig 1. This holder is somewhat easier to operate
than the one first discussed. A series resistance, which consisted
of a water-cooled stainless steel tube of 1Ω total resistance was
connected in the arc circuit to regulate the current. By means

2

of a sliding contact it was possible to regulate the effective resistance continuously on it. The source of voltage was a 34 kw dry rectifier. The arc was ignited each time with a high voltage impact. Figure 2 shows the arc in operation, ready for a spectrographic measurement. The natural radiation of the arc reaches the spectrograph slit through an iris diaphragm inserted in the window visible on the right hand side. On the left hand side of the arc a source of adjusting light may be seen.
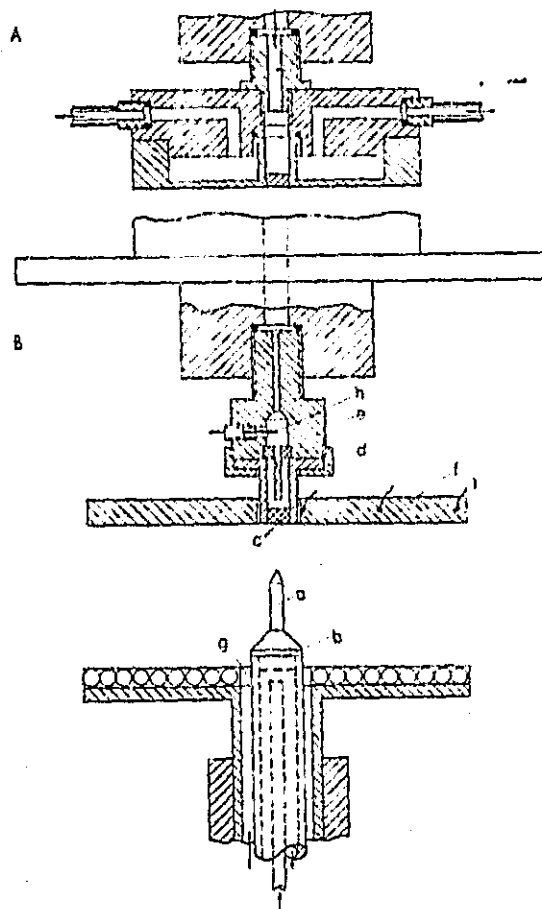

Figure 1

Arc equipment

A. With graphite anode holder
B. With water-cooled anode holder

    a. tungsten cathode
    b. cathode holder
    c. anode
    d. anode holder
    e. anode head
    f. protective plate
    g. ring channel
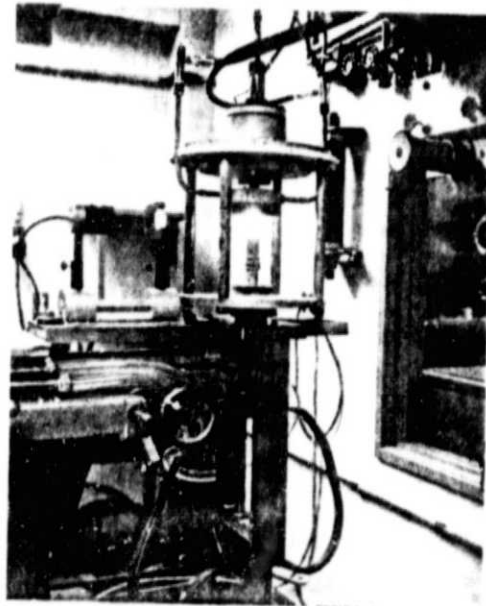   h,i.thermocouple elements

Figure 2.   Arc apparatus in operation

The Figures 3 to 5 show photographs of the arc for different
cooling gas flows, electrode distances and current intensities.   For
comparison Figure 5 also shows an arc, which burns between a
tungsten cathode and a water-cooled copper anode.   The magenetic
lines of force surrounding the arc and the electrical arc generate
electromagnetic forces (Lorentz forces) which near the cathode
because of the conical shape of the arc have components in the direc-
tion of the arc axis [2,3].   Thus a gas flow is produced, which is
to be directed on the anode at considerable velocity and which for
its part affects to a considerable extent the shape of the arc.
In Figures 3 to 5 this cathode beam meets the cooling gas flow
emerging from the porous cathode.   The flow conditions are shown once
again schematically with a solid line on Fig 7.   We will return later
to its effect on the thermal conditions in the anode.

Calorimetric Measurements

The measurement program included the following quantities;
surface temperature of the anode, amount of cooling gas, arc current
and arc voltage and temperatures in the arc.   The surface of the
anode was measured with an optical pyrometer.   It was found that the
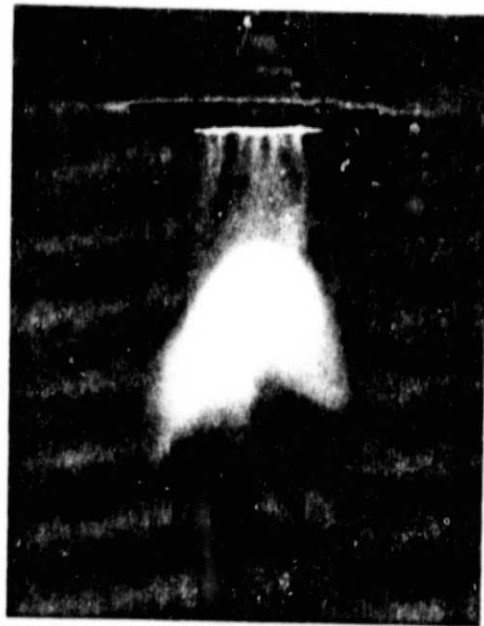
4

Figure 3.   S = 12.5mm, I = 100A, m/F = 0.9492g/s cm^2

Figure 4.   s = 3.75mm, I = 200A, m/F = 1.3560g/s cm^2
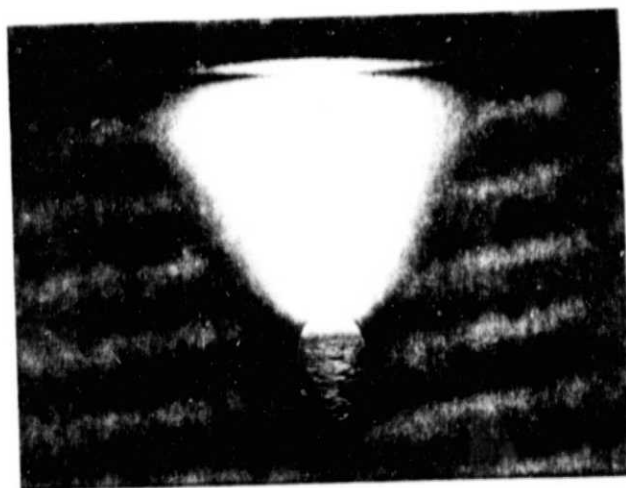
Figure 5. s = 15mm, I = 200A, m/F - 1.2363 g/s cm^2
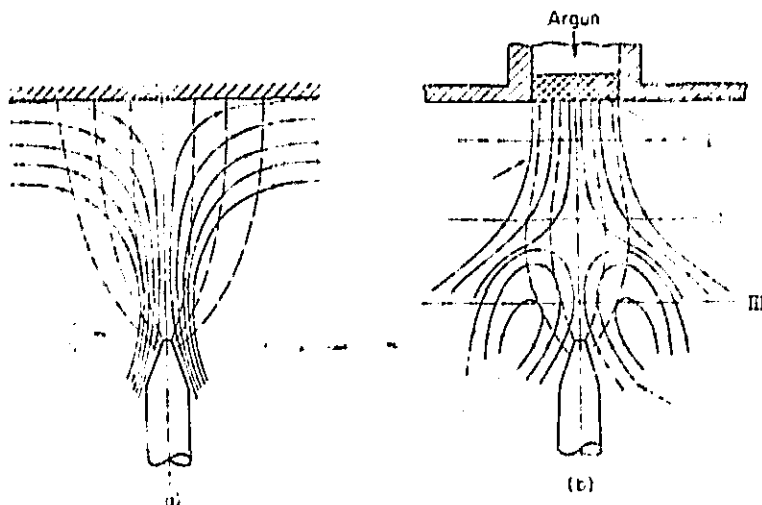

Figure 6. s = 6mm, I = 100A, water-cooled anode

Figure 7. Mass-current lines and electrical field lines in
the arc with water-cooled anode (a) and with gas-
cooled anode (b). I,II,III cross-sections
of the spectrographic temperature measurement.

portion of the anode, through which the electrons enter (anode
spot) has a practically constant local temperature. This anode spot
generally does not cover the total anode surface. Outside the spot,
the temperature decreases in the radial direction. Table 1 contains
the measurement results for the different series of experiments.
The results of several experimental series were given in reference
$\underline{/4/}$. T_1 is the temperature of the anode spot, T_2 is the average
temperature of the anode surface outside the spot. The size of the   /298
anode spot was determined visually. The ratio of the spot area to
the total anode area is designated by X in Table 1. The temperature of
the external surface of the anode holder was measured in several points
(See Fig 8), also with the pyrometer. The results of the measurements
are given in Fig 8. The mass flow ṁ of the cooling gas was determined
with a flow gauge. It is given in the first column of Table 1. The
second column gives the mass flow per unit of area ṁ/F of the anode
surface. The temperature of inflow of the cooling gas to the anode
was measured with a thermocouple (h) (Fig 1). The temperature T_0
fluctuated for the experiments by about 1 degree around the value 38°C.
The electrical current I was measured with an amperometer through
a secondary connection. It was kept constant for one series of experi-

7

ments. The electrode voltage was measured with a tube voltmeter
(Table 1). A certain irregularity is found in the variation of the
voltage values. These were caused by spontaneous melting or evaporation
of electrode material. Generally measurement series which were
extended over a very large area of the cooling gas flow, showed a
slight increase of the voltage U with increasing amount of cooling gas.

TABLE I

Carbon-Anode Holder (1 = 5mm, s = 12.5mm, I - 100A)

$\dot{m}$ (g/s)	$\dot{m}/F$ (g/s cm²)	U (V)	Q_u (kW)	T_1 (°K)	$T_.$ (°K)	x	Q_v (kW)	$Q_.$ (kW)	$Q_.$ (kW)	$\bar{p}$ (m/s)	ζ	Q_u/xF (kW/cm²)	I/xF (A/cm²)	$\dot{m}x$ (g/s)
0,4347	0,3444	23,5	2,35	2811	2200	0,9	0,55	0,33	0,250	17,7	0,25	1,10	88,0	0,3912
0,5796	0,4584	26,5	2,65	2811	2200	0,8	0,71	0,31		23,2	0,21	1,30	99,0	0,4637
0,7244	0,5737	25,0	2,50	2756	2200	0,7	0,85	0,27		27,4	0,21	1,60	113,1	0,5071
0,8694	0,6862	31,0	3,10	2589	2089	0,7	0,98	0,21		31,1	0,15	1,68	113,1	0,6086
1,0143	0,8015	22,5	2,25	2700	2144	0,5	1,10	0,21		35,7	0,20	2,56	158,3	0,5071
1,1592	0,9168	22,0	2,20	2756	2256	0,5	1,31	0,23		42,4	0,22	2,92	158,3	0,5796
1,2978	1,0280	22,5	2,25	2756	2200	0,3	1,38	0,19		44,8	0,20	4,95	263,9	0,3893

Spectrographic Measurement of Temperature

To obtain the temperatures in the arc gas, the arrangement
shown above in Fig 1 with water-cooled anode holder was used. The
evaluation of the spectrographic photographs assumes rotational
symmetry. Of several photographs those were selected in which this
condition was best satisfied. The temperatures in the arc given below
were measured for a current intensity of 200A, an electrode distance
of 15 mm and a cooling gas flow of $\dot{m}/F$ = 1 g/s cm^2.

The spectrographic investigations were carried out with a two-
meter two-grid spectrograph of the Bausch and Lomb Company. For
reasons of image representation techniques it was necessary to dis-
mantle one of the two grids and to mount the remining one in the
optical axis. The image of the vertically burning arc was formed
by an achromatic system (f:400mm) on the spectrograph slit and a
proportion 1.1:1. A reversing mirror connected in-between turned the
image by 90°, so that it came to lie horizontally on the slit. Figure
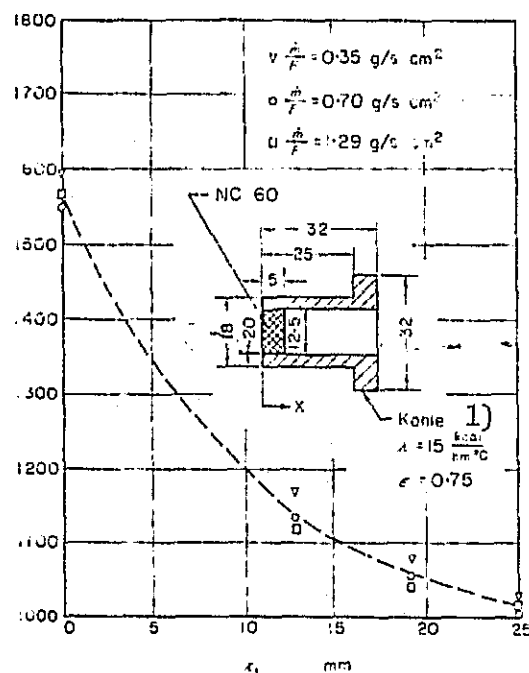9 shows the optical experimental equipment in a schematic manner.

Figure 8. Surface temperature on the anode holder
Key: 1) Carbon

The arc equipment was mounted on the bed of a heavy grinding
machine (Fig 2), so that the arc could be adjusted in three dimensions
with regard to the optical axis of the spectrograph. By vertical
adjustment of the equipment, the image of the arc was shifted sideways
in front of the spectrograph slit, and the arc cross-section to be
studied was adjusted. We give below the results of evaluation for two <u>/300</u>
cross-sections, shown in Fig 7. The first cross-section (I) is 2.5mm
under the anode surface, the second (II) in the center between anodes
and cathodes.

Kodak 1 N spectrographic plates were used for the photographs.
The spectral sensitivity of the plates used was determined by means
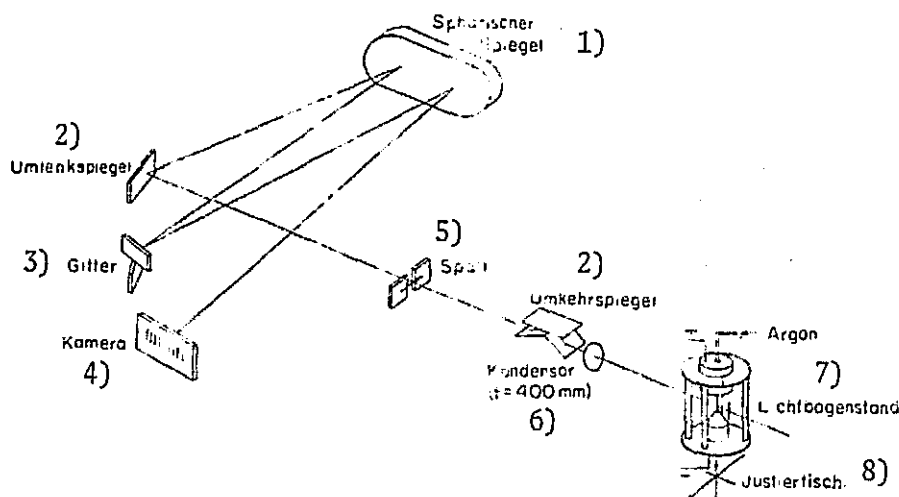of the carbon arc standard described by Euler /5/, whose spectrum was

9

Figure 9.   Schematic representation of the Bausch and Lomb two-grid
spectrograph with arc equipment

Key: 1) spherical mirror   5) slit
       2) deflecting mirror   6) condenser
       3) grid   7) arc level
       4) camera   8) adjusting table

graduated with a 7-stage filter of the Jarrel-Ash Company.   Figure
10 shows in the lower portion of the spectrum of the carbon arc standard.
The measured relative intensities of the wave length region from
7400Å to 8200Å overlapped with the actual relative radiation inten-
sities of the Euler arcs, so that a correction of the line intensities
obtained from the blackenings of the plate was superfluous.   The most
favorable lighting times were obtained by lighting tests of 1/30 to
1/40 s.   The light plates were developed for two minutes with Kodak D-19
developer at 20°C temperature and then further processed normally.

In addition to the carbon arc standard, figure 10 shows three superimposed
argon spectra, which correspond to the three arc-cross-sections studied.   The lines used
for the evaluation are characterized by arrows.   Figure 11 is a
spectrographic photo in the direction longitudinally to the arc axis
with wide slit.   Blackening and width of the atomic and ionic lines

indicate temperature distribution along the arc axis. The appearance
of ion lines shows high temperatures in the vicinity of the cathode.
The characteristic lines are identified in the longitudinal spectrum
in Fig 11. The Fe-arc spectrum is used only to identify the unknown
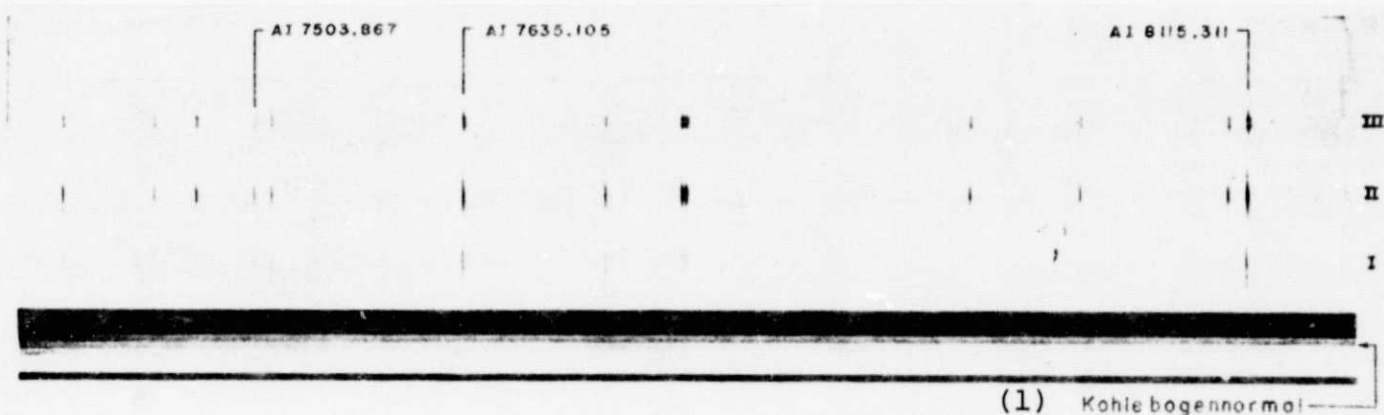lines in the gas-cooled light spectrum.

Figure 10. Transversal spectra in the arc cross-sections I,II,III
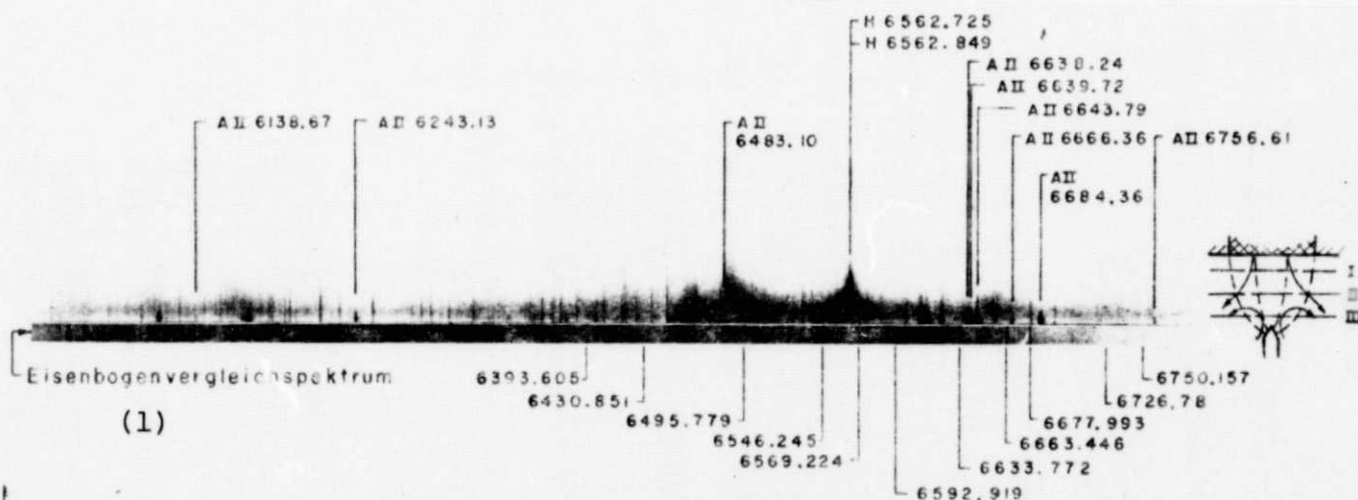and carbon arc standard
Key: 1) carbon arc standard

Figure 11. Longitudinal spectrum taken with 50μ slit width and
iron arc reference spectrum
Key: 1) iron arc reference spectrum

11

Evaluation of Experiments

Evaluations of the Calorimetric Experiments

From the above-described measurements thermal balances may be established for the arc and for the anode. The electrical power converted per unit of time is:

$$Q_0 = UI. \tag{1}$$

The amount of heat Q_k, which is absorbed by the cooling gas in the passage through anode and carried back to the combustion area was determined from the measured anode surface temperatures and the corresponding amounts of gas flowing through. It was assumed that on the anode surface, the gas temperature is equal to the anode temperature, which is justified because of the small pore diameter. It was moreover assumed, that the specific mass flow $\dot{m}/S$ is constant over the entire anode surface. In reality in the focal spot, because of the higher temperature prevailing there (higher viscosity of the gas) it is somewhat smaller than in the cooler area not affected by the arc current. According to approximate calculations, the last effect causes only a negligible error of a few percent in the calculated amount of heat Q_k. The latter was obtained with the following equation:

$$Q_k = \dot{m} [x \cdot (i_1 - i_o) + (1 - x)(i_2 - i_0)]. \tag{2}$$

The indices of the gas enthalpies I indicate the corresponding gas temperatures of the focal spot, in the external zone of the anode and before the entrance of the gas into the anode.

The heat radiation of the porous anode surface:

$$Q_q = \epsilon \cdot \sigma \cdot F [xT_1^4 + (1 - x) T_2^4] \tag{3}$$

where ϵ indicated the emission ratio of the anode surface, with σ as the Stephan-Boltzmann constant, and F designating the anode surface. The emission ratio of graphite was determined by Sieber [6] and ϵ equals 0.78. Euler [5] found similar values. The heat flow Q_1 transferred from the anode disk to the anode holder is emitted partly from the external surface F_h of the anode, partly dissipated through annular cross-section of the anode holder in the actual direction (Fig 8) and transferred to the anode heads. A third component, which

12

is carried away to the cooling gas by the internal wall of the anode holder, is carried with the cooling gas into the combustion area and should be not included with Q_1. The heat flow Q_1 is thus

$$Q_1 = \epsilon \cdot \sigma \int T^4 \, dF_h + \lambda \, (dT/dx) \, F_q \tag{4}$$

T indicates the surface temperature of the anode holder, F_q is cross-section area and λ the thermal conductivity of graphite. The second term in equation (4) is small in the present experiment as compared with the first term, therefore an approximate determination of the temperature gradient dT/dx from Fig 8 is sufficient. From the temperature of the aluminum disk (f) measured with the thermo-couple element (i) it is found, that reflection in the anode holder was negligibly small. It is possible to calculate with the heat balance

$$Q_g = Q_s - Q_1 + Q_q \tag{5}$$

Qg is a quantity which represents the energy remaining after subtract-ing the anode losses. These include among other things the cathode losses which according to earlier experiments came to less than four percent.

With the above thermal flows it is possible to establish a loss coefficient of the anode.

$$\zeta = \frac{Q_s + Q_1}{Q_a}. \tag{6}$$

The amount of energy Q_a transferred from the arc to the anode consists of the amount of heat absorbed by the cooling gas in the anode and the anode losses according to the relationships

$$Q_a = Q_K + Q_s + Q_1 \tag{7}$$

The heat flows and the anode loss coefficients are given in Table I for different amounts of cooling gas.

The heat flows can be clearly followed in the picture of the heat flow in Fig 12. It may be seen how the greater portion of the heat given off from the arc to the anode is transferred by the cooling gas back to the combustion area. The heat loss of the gas-cooled anode is 20 percent of the arc power (Fig 12). On a free burning arc with water-cooled anode (Fig 6) according to other published measurements, for

otherwise similar operating conditions, nearly 80 percent of the electrical energy was given off to the cooling water of the anode.

In the previously described experiments the decrease of weight of the porous anode was less than 0.1 grams per hour.

Evaluation of the Spectrographic Photographs

To evaluate the spectrographic photos it is assumed that in the gas-cooled arc column, thermodynamic equilibrium prevails locally. In this case the reaction equilibria between atoms, ions and electrons, as well as thermodynamic material values (viscosity, thermal conductivity diffusion coefficient) are clear functions of pressure and temperature. The assumption of local thermodynamic equilibrium applies in the arc column of arcs burning under atmospheric pressure with approximation as is shown by many investigations carried on such arcs [7]. The intensity
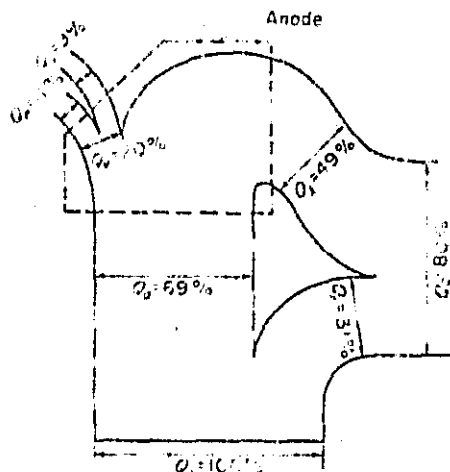

Figure 12. Picture of the heat flow of the anode, Q_g is the perceptible heat in the arc plasma plus about 4% cathode losses Q_r residual heat. $Q_v = Q_s + Q_i$ anode loss.

I_L of a spectral line of the light emission from the optically thin
layer of the arc is then related with the temperature T as follows:

$$I_L = \frac{1}{4\pi} \cdot A_4^m \cdot n_u \frac{g_4}{Z_0^{(i)}} \cdot$$
$$\exp(-E_m/kT) \cdot h \cdot \nu \cdot L \qquad (8)$$

The symbols used are clarified in the list of symbols. This equation
was applied for two spectral lines of the same particle. If the factor
common for two lines is designated

$$k = \frac{n_0 \cdot h \cdot L}{4\pi \, Z_0^{(i)}} \qquad (9)$$

we obtain by establishing the logarithm and conversion

$$\log \frac{I_L}{A_4^m \cdot g_4 \cdot \nu} = \frac{E_m}{k} \cdot \frac{1}{T} + \log k . \qquad (10)$$

Using equation (8) to obtain the local temperature in the arc, care
must be taken that in this case the radiation of the individual lines
comes from an inhomogeneous temperature field. Each beam which
passes through the spectrograph, consists of radiation from different
areas of the arc. This may be discussed on the basis of Figure 13,
in which the circle represents a cross-section through the arc. A
light beam which passes through the arc at the distance ξ from the
arc axis, carries all the radiation which is emitted along this
section, to the spectrograph. If the intensity of the line which is
emitted at the distance r from the arc axis is designated by $I_L(r)$, the
line intensity, which is observed from the spectrograph by means of the
photographic plate becomes

$$I_L(\xi) = \int I_L(r) \cdot d\eta$$

with $\quad d\eta = \frac{r}{\sqrt{(r^2 - \xi^2)}} dr \quad$ we obtain

$$I_L(\xi) = 2 \int_0^R \frac{I_L(r) \cdot r \cdot dr}{\sqrt{(r^2 - \xi^2)}} \qquad (11)$$
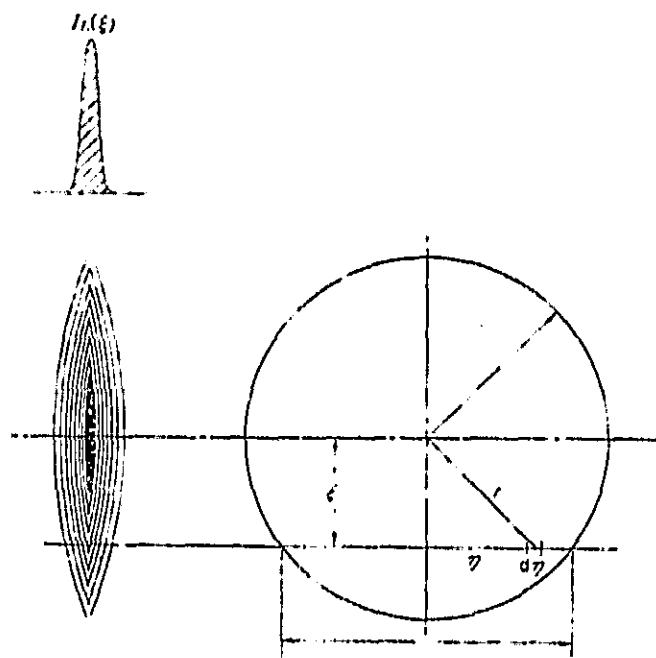
15

Figure 13.   Scheme of the spectrographic evaluation

The intensity of $I_L(\xi)$ can be determined from the spectro-photograph of a line.   Such a line is shown schematically on the left in Fig 13.   The blackening of the line at the distance ξ was measured with a densitometer.   The individual blackening values were then converted into intensity ratios by means of the blackening curve obtained from the carbon arc standard, and they were finally plotted over the line width.   The last stage is indicated schematically in the upper portion of Fig 13.   The area under the curve is proportional to the quantity $I_L(\xi)$.   By means of the Abel integral transformation /303 (11) now $I_L(r)$ can be calculated.   The calculation was carried out on an electronic computer (Univac Model 1103) in such a way that the integral of the equation (11) was converted into a summation with 24 finite steps.

The evaluation was carried out for the two neutral argon lines with wave length 8115.311Å and 7503.867 Å.   By forming the difference of equation (10) for the two lines it is possible to eliminate the constant K and thus calculate the temperature T(r) assuming that the other values occurring in the equation are known.   The absolute

transition probability A_n^m has, according to information provided kindly by private communication from Dr. H. Olsen of the Linde Company, Indianapolis/Ind. the values:

$$A_n^m \; 8115.311 = 1.5 \times 10^7 \, s^{-1}$$
$$A_n^m \; 7503.867 = 4.2 \times 10^7 \, s^{-1}$$

All other values were taken from the tables published by Moore. [8]. The temperature for profiles obtained in this way are shown in Fig 14 for the arc cross-sections I and II.
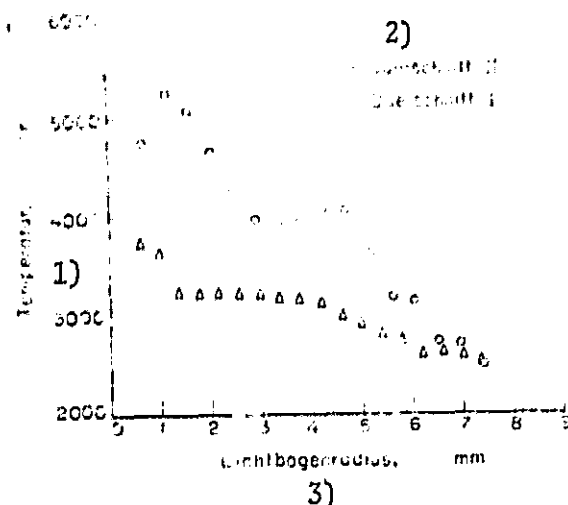
Figure 14. Temperature profiles in the arc cross-sections I and II.

Key: 1) Temperature
      2) Cross-section
      3) Arc radius

Discussion of the Experimental Results

The determination of the heat flow Q_a from the arc to the unknown allows the calculation of a specific heat flow Q_a/xF per unit of area of the anode focal spot. For conditions in Table I the heat flow load of the unknown fluctuates between 1.10 and 4.95 kW/cm^2, therefore reaches values which occur only in rare cases in technology. On water-cooled anodes, heat loads of the same order of magnitude were measured [9,10]. This makes it understandable, that a permanent operation of plasma generators with electrical arc raises difficultes with regard to the burning off of the water-cooled anodes, and the heat losses are extraordinarily high on the anodes. The gas cooling of the anode does not reduce indeed the heat load under all circumstances, as may be seen in comparing the values given in references

$\underline{/9/}$ and $\underline{/10/}$, but most of the energy transferred in the anode is carried back to the combustion chamber by the cooling gas. Through regenerative process the anode losses may be reduced to about 20 percent of the electrical arc power.

It is also interesting that the amount of cooling gas $\dot{m}x$, which flows through the spot of the anode, remains approximately constant independently of the cooling gas flow $\dot{m}$. The arc seems therefore to create itself the most favorable temperature of the spots by regulating the size of the spot. This temperature is so high, that porous metal anodes are destroyed by melting on the spot.

A quantitative study of the physical processes which caused the heat flow on the anode must be postponed until other more detailed measurements are available (electrical field intensity, size of the anode drop). A quantitative consideration can however be carried out on the basis of the existing results and a thorough investigation of the arc with water-cooled copper anode $\underline{/9,10/}$ to this end let us first consider the conditions in the arc with water-cooled anode.

The electrical current is carried in the arc by the electrons emerging from the cathode and entering the anode. As a result of the presence of the electrical field with regard to the gas filling $\underline{/304}$ the space between the electrodes, we have an average velocity v^-, the so-called drift velocity. This process may be compared with a diffusion process. The drift velocity has according to gas kinetic calculations $\underline{/9/}$ in an argon arc, an order of magnitude of 300 to 1000 m/s. As a result of the space charge connected with it, the electrons would require an enormously large drop of voltage between the electrodes, if the space charge was not compensated by positively charged ions. The ions are produced by thermal ionization of the gas as a result of the high temperature. The field intensities measured in the arc column are such that the gas there must be practically neutral, that means that the number of electrons n^- per unit of space must be equal to the number of the ions n^+ per unit of space. The ions have because of the electric field also a drift velocity of v^+ with regard to the gas, which is directed towards the cathode. This velocity is however much smaller because of the low velocity of the ions as compared with the electron mobility. According to gas kinetic calculations $\underline{/9/}$ v^+ is of the order of magnitude 1 m/s.

18

It was already mentioned earlier that in the gas filling the arc area, a mass flow also exists as a result of the Lorentz forces /3/. The corresponding mass velocity v is directed mainly in the arc column from the cathode to the anode. This velocity v is according to reference /3/ and /9/ of the order of magnitude 100 m/s. Thus we obtain for the velocities of the electrons and ions the following conditions with regard to the electrodes. The electrons move with a velocity of the order of magnitude $v^- + v$ to the anode. The drift velocity v^- is large as compared with the mass velocity v. The average trajectory lines of the electrons are therefore only influenced little by the mass flow. Figure 7 shows these trajectories plotted in dash-lines. The velocity of the ions with regard to the electrodes is of the order of magnitude $v - v^+$. The drift velocity v^+ of the ions is very low as compared with the mass velocity v. The ions are therefore mainly carried with the mass flow from the cathode region towards the anode. Therefore in rough outlines the conditions may be illustrated by the superimposition of two flows: the mass flow of an ionized gas with a current line field, as shown in Fig 7 in solid lines, and the flow of an electron gas with a source in the cathode surface and a depression in the anode surface. The similarity with a diffusion process is further emphasized.

The conditions may be rendered somewhat clearer by a quantitative consideration. Here we will limit ourselves to the average conditions in the arc column, therefore be satisfied with a unidimensional study. The particle density n^- of the electrons is according to what was stated above practically equal to the arc column to the particle density n^+ of the ions.

$$n^- = n^+$$

(12)

Let $\dot{n}^-$ be the particle flow of electrons per unit of area and time. This flow contains not only the electrons emerging from the cathode, but also those formed by ionization in the vicinity of the cathode. Let the latter be called "secondary" electrons, and let their particle current density be $\dot{n}_s^-$. Since the latter are formed from neutral atons, we have

$$\dot{n}_s^- = \dot{n}^+$$

(13)

if $\dot{n}^+$ in the case the particle current of the ions per unit of area.
Moreover we have

$$n^- = n^-(v^- + v) \tag{14}$$

$$\dot{n}^+ = n^+(v - v^+) \tag{15}$$

From the four above equations it follows that

$$\frac{n^-}{\dot{n}_i^+} = \frac{v^- + v}{v - v^+} \tag{16}$$

or approximately

$$\frac{\dot{n}^-}{\dot{n}_i^+} = \frac{v^-}{v} + 1 \tag{17}$$

since v^+/v is small as compared with 1. From the earlier given data
on the values of the individual velocities it follows, that the total
electron current is about 4 to 11 times as large as the current of the <u>/305</u>
"secondary" electrons.

In the vicinity of the cathode, conditions prevail which we can
now explain in a simplified manner by the superimposition of two
flow processes, a mass flow of a ionized gas with a nature of stagnation
point flow (Fig 7) and the falling flow of an electron gas, which
contains the electrons closing the circuit. The heat transfer to the
mass flow may be calculated with good approximation, since the gas
is only slightly ionized and consequently the lowest number does not
deviate too much from the value 1 /11/. The calculation shows that
about 15 to 25 percent of the total heat flow Q_a is carried to the
anode by convection through the mass flow to the water-cooled copper
anode. The electron gas carries its total enthalpy (consisting of
internal energy and kinetic energy) to the anode and gives off moreover
an amount of energy to the anode, which is released in the entrance into
a solid body, the electron entrance work (similar to the condensation
energy). If the enthalpies are calculated from the temperature of the
arc column in the vicinity of the anode and from velocity $v^- + v$,
we obtain for the heat flow given off by the electron gas to the anode
surface as about 50 percent of a total heat flow Q_a. The remaining 25
to 35 percent are caused by the following processes. The mass flow
towards the anode implies a boundary layer which in the present
conditions is about 1mm thick. Within this boundary layer the tempera-

20

ture drops from the value inthe arc column (about 12000°K) to the value
of the anode surface. Accordingly the degree of ionization correspond-
ing to thermal equilibrium also drops. On the other hand, however,
the electron flow must be maintained. This means either an increased
drift velocity of electrons according to equation (14) or an electron
density which is larger than the ion density or field ionization. Each
of these possibilities requires however, an increased field intensity.
Actually in the vicinity of the anode the so-called anode drop is
observed, which requires a field intensity which is much larger than
that in the arc column. This implies a production of heat (Joule heat),
which is limited to the immediate vicinity and is therefore given off
practically totally to the anode. It can thus be calculated from the
mentioned value that the electrical current and the voltage drop in the
anode drop region.

Now it should be possible to study how far the conditions are
different in the gas-cooled porous anode. The mas flow is basically
altered as shown by Fig 7. The ion flow is essentially like the mass
flow. But now in the vicinity of the anode there must be a source
of ions instead of an ion trap. The convective heat transfer through
the mass flow is certainly greatly reduced just like the case of
transpiration cooling of a wall (10). The flow of the electron gas
is affected by the mass flow only indirectly, that is through the
temperature field. Thus essentially the heat flow transferred through
the electron gas to the anode is altered to the extent to which the
temperature in the vicinity of the anode and the electron entrance
work are different. The internal heat production in the form of Joule
heat depends on the final run on the electrical drop of voltage in the
region of the anode fall.

The temperature profile reproduced in Figure 14 shows a gradual
increase in the gas temperature in the direction from the anode surface
towards the cathode. The conditions are different in the water-
cooled copper anode, where a greater increase in the temperature was
measured in a layer only about 1mm thick. In the evaluation of the
temperature it must be recalled that argon contains traces of carbon
vapor when emerging from the anode. It is possible that the electron
temperature is higher than the gas temperature at least in the cross-
section I. The nonuniform variation of the temperature profile in

the cross-section II indicates that in this mixed zone considerable deviation from axial symmetry occur. The spreads occurring in the evaluation of the spectral lines in the cross-section III were so large that they made it impossible to determine the temperature profile, but the position of the line intensity maxima outside the arc axis allows the conclusion to be drawn that in this cross-section temperatures of at least $15000^{O}K$ prevail.

Literature

1. C. Sheer, <u>Vitro Laboratories Report</u> (1959).

2. K. Larche, <u>Lichttechnik</u> 2, 41 (1951).

3. H. Maecker, <u>Z. Phys</u>. 414, 198 (1955)

4. P. Scheock and E.R.G. Eckert. <u>Proc.of the 1961 Heat Transfer and Fluid Mechanics Institute</u>, Stanford University Press (1961).

5. J. Euler, <u>Ann. Phys</u>. II, 203 (1953).

6. W. Sieber, <u>Z. Tech. Phys</u>. 22, 130 (1941).

7. W. Finkelnburg and H. Maechker, <u>Handbuch der Physik</u> (Handbook of Physics) Vol. XXII, 255 (1956).

8. Ch. E. Moore, Atomic Energy Levels, <u>National Bur. Stand. Circular</u> 467 (1949).

9. P.A. Schoeck, Ph.D. Thesis, University of Minnesota (1961).

10. P.S. Schoeck and E.R.G. Eckert, To Appear in Volume II of <u>Proc. of International Congress on Ionization Phenomena in Gases</u> (1961). North Holland Publishing (1961).

11. R.S. Brokaw, Personal communication.

12. Ernst Eckert, <u>Einfuehrung in den Waerme und Stoffaustausch</u> (Introduction into Heat and Substance Exchange) Springer Verlag, Berlin (1959).